International Conference on Space Optics—ICSO 2010

Rhodes Island, Greece

4–8 October 2010

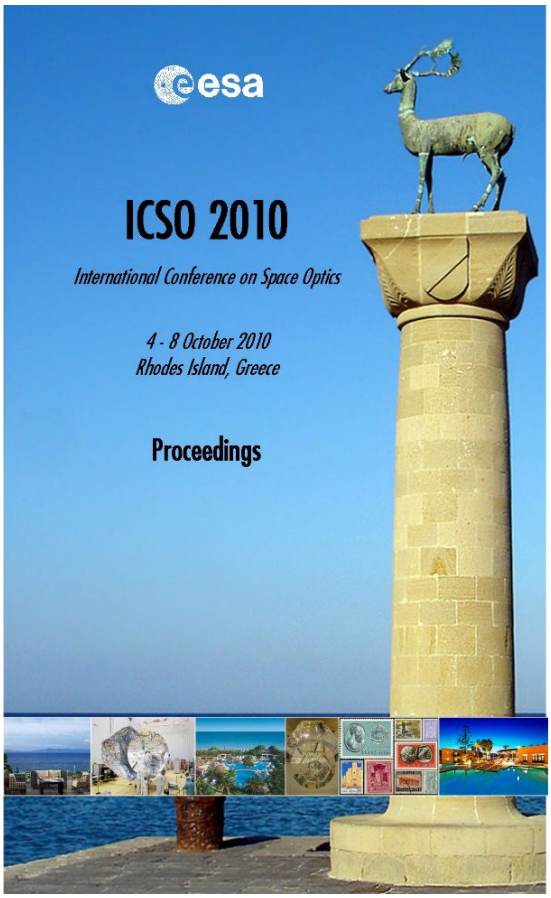

Edited by Errico Armandillo, Bruno Cugny, and Nikos Karafolas

Experimental demonstration of 1.5Hz passive isolation system for precision optical payloads

Xin Guan, Guang-yuan Wang, Dong-jing Cao, Shao-fan Tang, et al.

International Conference on Space Optics — ICSO 2010, edited by Errico Armandillo, Bruno Cugny, Nikos Karafolas, Proc. of SPIE Vol. 10565, 105651Q · © 2010 ESA and CNES
CCC code: 0277-786X/17/$18 · doi: 10.1117/12.2309112

EXPERIMENTAL DEMONSTRATION OF 1.5HZ PASSIVE ISOLATION SYSTEM FOR PRECISION OPTICAL PAYLOADS

Guan Xin[1], Wang Guang-yuan[1], Cao Dong-jing[2], Tang Shao-fan[2], Chen Xiang[2], Liang Lu[1], Zheng Gang-tie[1]
[1] *School of Aerospace,Tsinghua University, China.* [2] *Beijing Institute of Space Mechanics & Electricity, China*

Contact Details
Mailing Address: School of Aerospace, Tsinghua University, Beijing, 100084, China
Email: guan-x07@mails.tsinghua.edu.cn

I. INTRODUCTION

The ground resolution of remote sensing satellite has been raised from hundreds of meters to less than one meter in recent few decades. As a result, the precision optical payload becomes more and more sensitive to structure vibrations of satellite buses. Although these vibrations generally have extremely low magnitude, they can result in significant image quality degradation to an optical payload. The suggestion of using vibration isolators to isolate payload from the satellite bus has been put forward in 1980s'[1]. Recently, WorldView-2 achieved its perfect image quality via using a set of low frequency isolators[2]. Recently, some of the optical payload manufacturers begin to provide vibration isolators as standard parts together with their main products .

During the prototype testing of an earth resource satellite, the image of the optical payload was found to jitter for 5~10 pixels due to disturbances transmitted from the satellite bus structure. Test results indicated that the acceleration level of the vibration was of mG magnitude. To solve the problem, a highly sensitive vibration isolation system was developed to reduce the transmission of disturbances. Integrated isolation performance tests showed that the image jitter can be decreased to below 0.3 pixels.

II. THEORY OF VIBRATION ISOLATION

Fig. 1. shows the dynamic model of the passive isolator. m_0 is the mass of the disturbance source, k_0 and c_0 represent the stiffness and damping respectively of the passive isolator. $p(t)$ is the force generated by the disturbance source and $f(t)$ is the force transmitted to the payload.

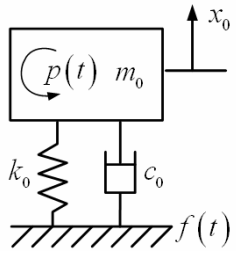

Fig. 1. Passive Isolation System

The dynamic equation of motion for this system is

$$m_0\ddot{x}_0 + c_0\dot{x}_0 + k_0x_0 = p(t) \quad (1)$$

Force transmitted to the payload structure is

$$f(t) = c_0\dot{x}_0 + k_0x_0 \quad (2)$$

Taking the Laplace transform on both side of Eq. (1), an expression for the vibration transmissibility can be obtained as

$$G(s) = \frac{F(s)}{P(s)} = \frac{c_0s + k_0}{m_0s^2 + c_0s + k_0} \quad (3)$$

With the definition of isolation frequency and damping ratio,

$$\omega_0 = \sqrt{\frac{k_0}{m_0}}, \quad \zeta_0 = \frac{c_0}{2\sqrt{m_0k_0}}$$

The transmissibility can be rewritten as

$$G(j\omega) = \frac{k_0 + j\omega c_0}{(k_0 - \omega^2 m_0) + j\omega c_0} \quad (4)$$

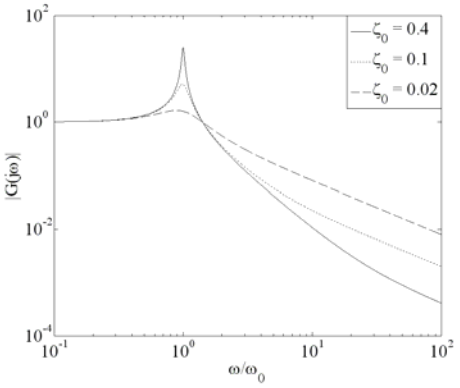

Fig. 2. Transmissibility of Passive Isolation System

Upon an examination of Fig. 2, it can be found that to achieve satisfactory vibration attenuation a vibration isolator should be designed with its cut-off frequency lower than the major frequencies of the disturbance forces. The damping coefficient of the isolator should also be selected to provide a proper compromise between amplification at the isolation frequency and attenuation at higher frequencies.

III. DESIGN OF MICRO-VIBRATION ISOLATOR

The on-orbit vibration of the satellite structure has a very low magnitude, and its typical acceleration and displacement levels are usually several mG and μ m respectively. There is no essential difference between these micro-vibrations and vibrations with large magnitude, but vibration isolators should be specially designed to meet the new requirements arisen from such extremely low amplitude.

Some existing vibration isolation devices consist of six actuators arranged in a geometrical configuration commonly known as Stewart platform and attached to the upper and bottom brackets through hinges. Clearance of several micrometers in the kinematic pair is necessary to ensure the expected form of motion. Nevertheless, in the case of micro-vibrations, such clearance may not only prevent the spring and damper from working normally but also result in unpredictable deviation of the isolation parameters from designed values. Flexure joints are utilized in some of the recent micro-vibration isolator designs to avoid the uncertainties induced by hinge clearance [3]. Furthermore, dampers using the viscous fluid should also be avoided because of some disadvantages such as difficulty to seal, insensitive to micro-vibration, and etc. A highly sensitive damper with excellent micro-vibration damping capabilities was developed using no other materials except metal.

As shown schematically in Fig. 3., the micro-vibration isolator consists of a damper made from metal damping material. Energy is dissipated in the shearing of the damper as the piston is pumped by the vibrational displacements. Meanwhile, recovery force needed in the isolation is obtained through the deformation of the damper together with the tuning spring. Here, the tuning spring is for adjusting the whole spring stiffness to compensate the manufacture deviation of the metal damper's stiffness. The nonlinear stiffness characteristic of the metal damping material can both provide the desired low stiffness for on-orbit micro-vibration isolation and also high stiffness necessary for surviving in the launch stage[4].

Additionally, through the design of the flexure joints at both ends, desired transverse stiffness of the isolator can be achieved. Consequently, four isolators can serve as an assembly to implement vibration isolation in all six DOFs.

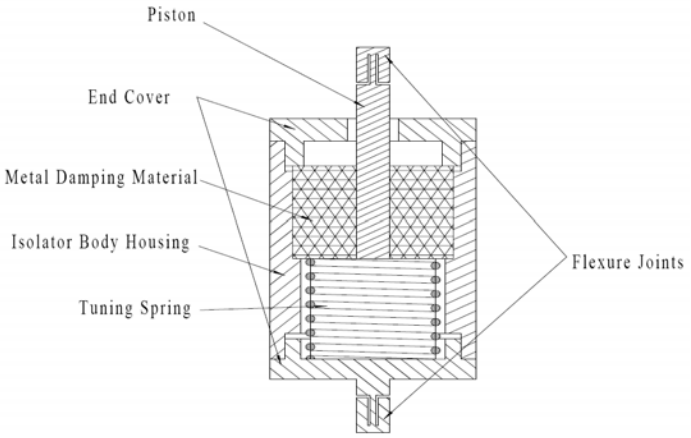

Fig. 3. Schematic of Micro-Vibration Isolator

IV. DESIGN AND SIMULATION OF THE ISOLATION DEVICE

Fig. 4 shows the design configuration of the isolation device. The payload is supported by four isolators, both the axial and transverse stiffness of which can be designed as described above.

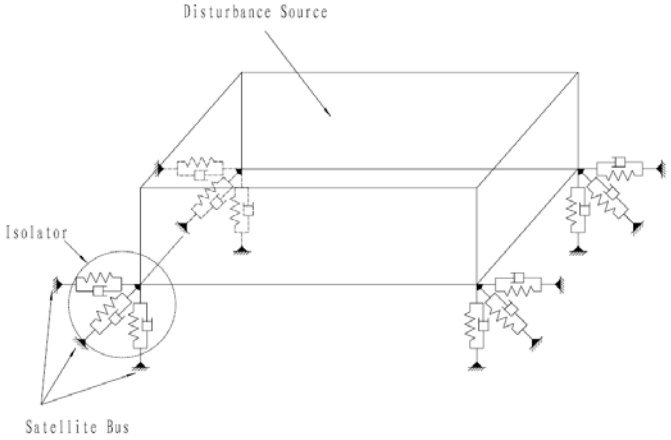

Fig. 4. Schematic of the Isolation System

To achieve sufficient attenuation in the major direction of the disturbance forces and meanwhile reduce the unexpected motion in other DOFs, a design of the isolation device is conducted according to the theory presented in Section 2. The resultant normal modes of the payload are as follows in Tab. 1.

Tab. 1. Normal Modes

Mode Description	Natural Frequency
Pitch	1.348 Hz
Roll	1.577 Hz
Vertical Translation	1.606 Hz
Horizontal Translation 1	2.847 Hz
Horizontal Translation 2	2.881 Hz
Yaw	3.973 Hz

A transient response analysis was carried out for the purpose of estimating the reduction in vibration magnitude due to the isolation. The finite element model of the satellite integrated with the model of the isolation system was used to perform the analysis. Time history of the acceleration response of the payload is plotted in Fig. 5, which shows that the amplitude of the response has been significantly attenuated. Compared to the non-isolated case, the RMS of the acceleration response was reduced by 99.4%.

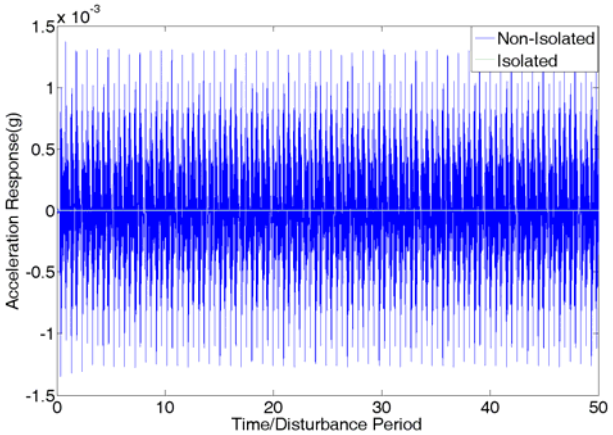

Fig. 5. Time History of Acceleration Response

V. INTEGRATED ISOLATION PERFORMANCE TESTING

A. Auxiliary Suspension System

Since the fundamental natural frequency of the isolation was around 1.5Hz, to avoid damage of the isolators, auxiliary suspension system must be adopted in ground isolation performance testing. This is also an important measure for simulating the zero-gravity environment on the orbit. Generally, to guarantee better testing results, the natural frequency of the suspension system should below 0.3Hz, i.e. 1/5 of the isolation system frequency. However, if tension springs were simply used to achieve this very low suspension frequency, the static deformation would be more than 3 meters, which would not be permitted by the actual condition of the laboratory. To overcome this problem, a nearly-zero Hertz suspension system was successfully developed, and a suspension frequency below 0.2Hz is achieved, which includes the contribution of electrical cables' stiffness.

B. Testing Configuration and Results

Payload module of the satellite was used in the integrated testing. A number of 3-axis accelerometers were arranged to ensure good surveillance of important positions on both the satellite structure and the payload. The testing was conducted in three different modes shown in Tab. 2.

Tab. 2. Testing Modes

	Disturbance	Isolation	Purpose
Mode 1	On	Off	Disturbance Characteristic
Mode 2	On	On	Isolation Performance
Mode 3	Off	On	Background Noise

Fig. 6 shows PSD of the acceleration response at one of the payload mounting points in the three testing modes described above. It can be seen that the two major contents of the disturbance were reduced by 99.5% and 99.9% respectively.

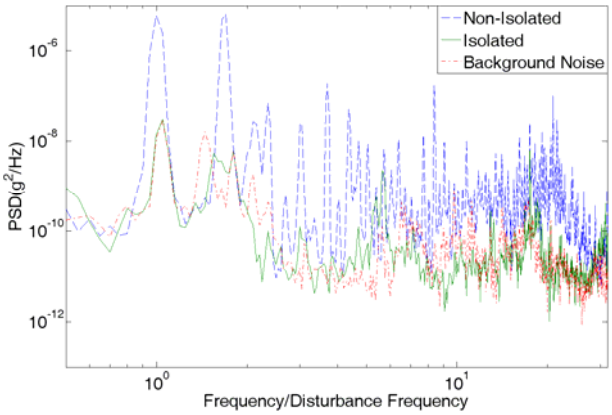

Fig. 6. PSD of Acceleration Response

Tab. 3. Attenuate Percentage of Disturbances

Measuring Points	First Major Content		Attenuate Percentage	Second Major Content		Attenuate Percentage
	Non-Isolated	Isolated		Non-Isolated	Isolated	
1	2.91E-06	1.92E-08	99.34%	3.83E-06	1.45E-08	99.62%
2	2.28E-07	3.73E-09	98.36%	1.48E-06	1.19E-08	99.20%
3	1.18E-07	3.75E-09	96.82%	1.47E-06	4.76E-09	99.68%
4	2.57E-06	1.74E-08	99.32%	3.48E-06	6.12E-09	99.82%
5	3.58E-08	1.00E-09	97.21%	7.83E-07	9.55E-09	98.78%
6	1.42E-06	7.48E-09	99.47%	1.62E-06	6.20E-09	99.62%
7	1.48E-06	9.59E-09	99.35%	1.45E-06	6.04E-09	99.58%
8	7.26E-08	1.17E-09	98.39%	5.47E-07	2.78E-09	99.49%

Fig. 7 shows time history of the acceleration response at one of the payload mounting points in the three testing modes.

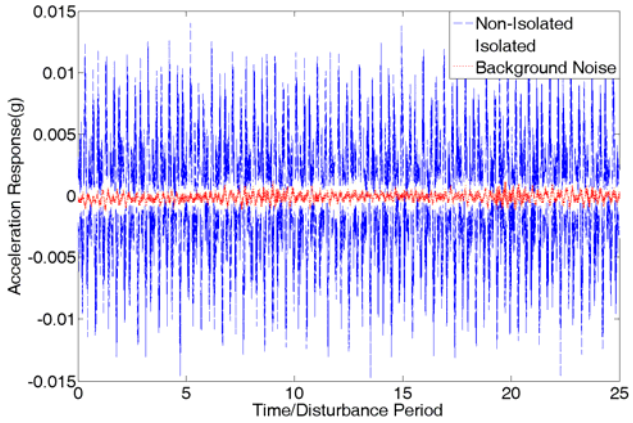

Fig. 7. Time History of Acceleration Response

The payload was imaging the scene simulator throughout the testing to evaluate the influence of both disturbances and the isolation device. As can be seen from Fig. 8(a), the image became contorted subject to the disturbances transmitted from the satellite bus structure. In a comparison, the image shown in Fig. 8(b) is resumed to be perfectly straight with the isolation device's functioning.

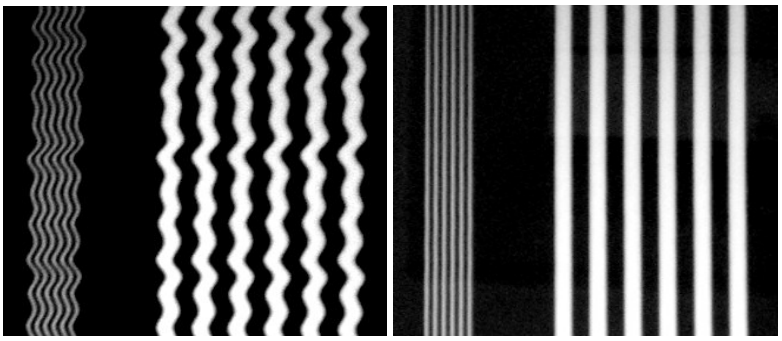

（a）Image without Isolation Device（b）Image with Isolation Device Working

Fig. 8. Image of the Optical Payload

C. Discussions on Testing Errors

- Background Noise

Background noise contributed 69%~99% to the RMS of the acceleration response when the isolation device was working, as shown in Tab. 4. Since there would be no ground vibration or any sensor noise when the satellite is working on-orbit, the performance of the isolation device will be better than that in the testing. Numerical calculation result indicates that the jitter will be below 0.3 pixels.

Tab. 4. Contribution of Background Noise to the Response

Direction	Background Noise(grms)	Response of Isolated System(grms)	Noise Ratio
x	2.2425e-004	3.2360e-004	69.30%
y	1.7080e-004	1.9288e-004	88.55%
z	3.2604e-004	3.2838e-004	99.29%

- Consistency between Ground Testing and On-Orbit Status

The integrated testing was conducted with the payload module rigidly attached to a cradle whereas there will not be any constraints to the satellite on orbit. A FEM analysis was carried out to evaluate the influence on the isolation performance caused by this difference in boundary conditions and structure configurations. Results show that the isolation device will perform well both on orbit and on ground.

As can be seen from Fig. 9 and Fig. 10, the shape of the time history response curve is similar while the amplitude of the on-orbit situation is a little bit lower compared to the fixed situation. Taking into account that there would be no air damping effect once the satellite is on the orbit, responses of the two situations should be of similar magnitude.

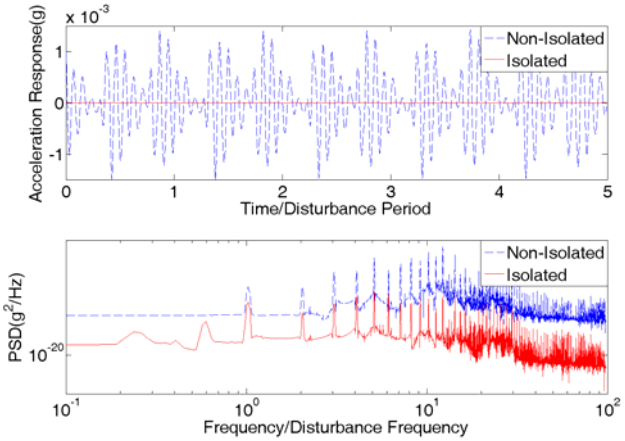

Fig. 9. Time History and PSD by FEM Analysis(Fixed)

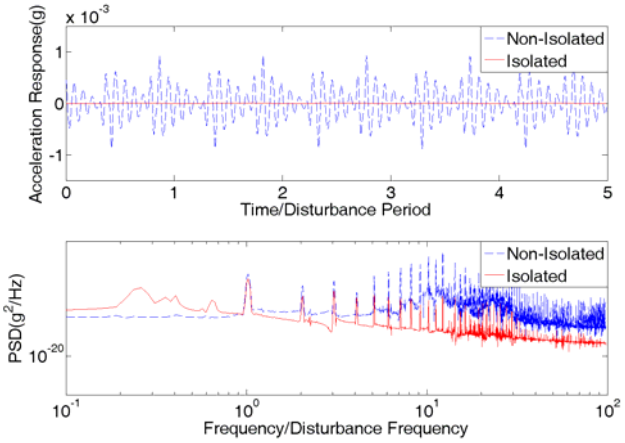

Fig. 10. Time History and PSD by FEM Analysis (On Orbit)

VI. CONCLUSION

A low frequency micro-vibration isolation system was developed to attenuate disturbances transmitted to the optical payload. Integrated testing results show that the image quality has been significant improved and the image jitter can be decreased to below 0.3 pixels (when the influence of background noises is removed). Numerical simulation results with FE model of the satellite indicate that the ground test with only payload module fixed to a cradle can well simulate the on-orbit situation of whole satellite.

REFERENCES

[1] R.A.Laskin, S.W.Sirlin, "Future Payload Isolation and Pointing System Technology", *J.Guidance*, vol.9, pp. 469-477, July-Augst 1986.

[2] "WorldView-2 Offers Unsurpassed Imaging Capabilities", *Earth Imaging Journal*, Online Version

[3] Virginio Sannibale, Gerardo G.Ortiz, William H.Farr, "A Sub-Hertz Vibration Isolation Platform for a Deep Space Optical Communication Transceiver", *Proc. Of SPIE*, vol.7199, 2009

[4] G.Y.Wang, X.Guan, X.Chen, S.F.Tang, L.Liang, "Parameter Design and Experimental Study of a Double State Nonlinear Isolator", in press.